Research on Engineering Structures & Materials
www.jresm.org
Research Group

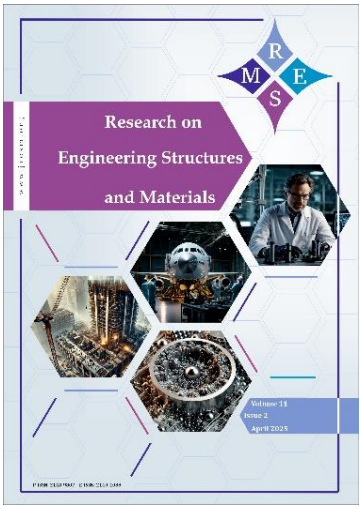

Effects of elevated temperatures on the stress-strain behavior and microstructure of normal and high-strength concrete

Amenah M. Abdulrazzaq, Haider A. Abdulhameed, Maan S. Hassan

Online Publication Date: 20 December 2025

URL: http://www.jresm.org/archive/resm2025-1260ic1013rs.html
DOI: http://dx.doi.org/10.17515/resm2025-1260ic1013rs

Journal Abbreviation: *Res. Eng. Struct. Mater.*

To cite this article
Abdulrazzaq A M, Abdulhameed H A, Hassan M S. Effects of elevated temperatures on the stress-strain behavior and microstructure of normal and high-strength concrete. *Res. Eng. Struct. Mater.*, 2026; 12(2): 931-942.

Research on Engineering Structures & Materials
www.jresm.org
MIM Research Group

Research Article

Effects of elevated temperatures on the stress-strain behavior and microstructure of normal and high-strength concrete

Amenah M. Abdulrazzaq [a], Haider A. Abdulhameed [*,b], Maan S. Hassan [c]

College of Civil Engineering, University of Technology- Iraq, Baghdad, Iraq

Article Info

Article History:

Received 13 Oct 2025

Accepted 15 Dec 2025

Keywords:

Fire resistance;
Stress-strain relationship,
Normal-strength concrete,
High temperature concrete,
Microstructural degradation

Abstract

This study investigates the stress-strain relationship and the microstructure, in addition to visual observations of color change, cracking, and spalling, of normal-strength concrete (NSC) and high-strength concrete (HSC) after exposure to various temperatures. An electric furnace was used to heat cylindrical specimens with dimensions of 100×200 mm to the temperatures of 400°C, 600°C, and 800°C to measure the mechanical and microstructural properties of concrete at those extremes. Both NSC and HSC maintain their structural integrity with slight surface damage at 400°C. By 600°C, thermal damage is clearer, with C-35 developing cracks and rough surfaces and C-55 showing signs of internal microcracking. NSC spalls and suffers significant surface cracking at 800°C, while HSC experiences internal damage because of its dense structure. Both compressive strength and axial strain results shown a significant degradation with increasing the temperature. The compressive strength decreased by 22.4%, 61.5%, 79.3%, at 400°C, 600°C, and 800°C; respectively. Regarding Stress-strain curves demonstrate reduced stiffness and strength as temperature increases. At 800°C, the strength and ductility of both types of concrete decreased significantly; HSC showed a greater reduction. These findings highlight the need for temperature effects to be accounted for in the design of structures made of concrete and subjected to high temperatures. This investigation can help with the design of structures that are resistant to fire and the evaluation of the structural integrity after exposure to fire.

1. Introduction

Concrete is extensively utilized as a principal structural element in buildings owing to its multiple advantages, including strength, durability, ease of manufacture, and no combustibility compared to other construction materials. Concrete structural members utilized in buildings must comply with the relevant fire safety regulations outlined in building codes. Fire constitutes one of the most extreme climatic situations that structures may encounter; hence, the implementation of adequate fire safety measures for structural components is a critical element of architectural design [1-5]. Fire resistance, defined as the duration a structural member maintains its integrity, stability, and temperature transfer capabilities, quantifies fire safety precautions for structural members. Concrete often has superior fire-resistant characteristics compared to any other building material [7]. The remarkable fire resistance of concrete arises from its basic materials, namely cement, and aggregates, which chemically mix to create an essentially inert substance characterized by low thermal conductivity, high heat capacity, and diminished strength degradation at elevated temperatures. The gradual rate of heat transmission and reduction in strength allows concrete to function as an efficient fire barrier, safeguarding both neighboring areas and itself from fire damage [8].

*Corresponding author: haider.a.abdulhameed@uotechnology.edu.iq
[a]orcid.org/ 0009-0009-4914-8966; [b]orcid.org//0000-0002-4138-4755; [c]orcid.org/0000-0002-5693-879X
DOI: http://dx.doi.org/10.17515/resm2025-1260ic1013rs

The concrete's mechanical, thermal, and deformation characteristics used to make a concrete structural element have an impact on how the element behaves when it is exposed to fire. Like other materials, concrete's thermal, mechanical, and deformation properties change significantly in the temperature range linked to structure fires. These characteristics depend on the composition and properties of concrete and change with temperature. Concrete's properties at room temperature and at higher temperatures are greatly influenced by its strength. When compared to (NSC), the characteristics of HSC show noticeable variation in temperatures. This variation is particularly significant for mechanical properties, influenced by strength, moisture content, density, heating rate and porosity [9].

In recent years, the adoption of numerical methods for calculating the fire resistance of structural components is increasing, as these methods are significantly more cost-effective and time-efficient. When a structural element experiences a specified temperature-time exposure during a fire, this exposure will result in a predictable temperature distribution within the element. Elevated temperatures induce deformations and alterations in the properties of the constitutive materials of a structural member. High temperatures significantly alter the chemical composition and physical structure of concrete. Dehydration, namely the release of chemically bonded water from calcium silicate hydrate (C-S-H), becomes substantial at temperatures beyond approximately 101°C [10]. The dehydration of hydrated calcium silicate and the thermal expansion of the aggregate elevate internal tensions, resulting in the induction of microcracks within the material at 300°C. Calcium Hydroxide [$Ca(OH)_2$], an essential compound in cement paste, dissociates at around 530°C, leading to the shrinkage of concrete [11]. The fire is often quenched with water, and CaO transforms into $Ca(OH)_2$, resulting in the cracking and crumbling of concrete. Consequently, the impacts of elevated temperatures are typically manifested as surface cracking and spalling [12]. Color alterations may also transpire during exposure [13]. The changes induced by elevated temperatures become more pronounced when the temperature exceeds 500°C. The majority of alterations observed in concrete at this temperature are deemed irreversible. C-S-H gel, the component responsible for the strength of cement paste, decomposes at temperatures exceeding 600°C. At 800°C, concrete begins to disintegrate, and beyond 1150°C, feldspar liquefies, leading to the transformation of cement paste minerals into a glassy phase. [12-15]. Consequently, significant microstructural alterations occur, leading to a loss of strength and durability in concrete.

This study aims to investigate the effect of different heat ranges on the stress-strain behavior and the microstructure affecting the NSC and HSC to provide valuable insights into their fire resistance and post-fire performance. Fire is a significant exposure hazard; therefore, the implementation of adequate fire resistance for structural elements is a critical safety criterion in the design of buildings. The fire resistance of structural members relies on the thermal and mechanical capabilities of the constituent materials at elevated temperatures. Temperature is an important factor that affects the strength and the stress-strain relationships of concrete. This study aimed to examine the impact of elevated temperatures on the strength and stress-strain relationship of (NSC) and high-strength concrete (HSC). Also, to further understand the effects of heat on concrete, microstructural analysis was conducted using Scanning Electron Microscopy (SEM) and X-ray diffraction (XRD).

2. Experimental Phase

To achieve the objectives of the study, laboratory concrete cylinders were produced in accordance with established standards, and evaluations were carried out to investigate the effects of elevated temperatures on the concrete properties, followed by an analysis of their behavior after cooling. This study's laboratory work was carefully divided into three parts, each of which was essential to the investigation's main goal. The first step included determining the mixture ratio, casting the concrete molds, and then allowing them to cure for 28 days. The specimens were heated to different temperatures in the second step. In the third stage, axial compression stresses are applied to concrete cylinders to evaluate the effects of heating. The parameters studied include the concrete type and various heating degrees, and the impact of these parameters on compressive capacity was analyzed.

2.1 Materials

Two concrete mixes with compressive strengths of 35 MPa, which represent NSC, and 55 MPa, which exhibit HSC, were made using ordinary Portland cement (Type I), natural fine aggregate with a maximum aggregate size of 4.75 mm, and crushed coarse aggregate with a maximum aggregate size of 13 mm.

2.2 Details of Specimens

Twenty-four specimens were made using cylinder molds measuring 100 by 200 mm. The selected dimensions were customized to accommodate the electric furnace, utilizing two varieties of plain concrete (NSC) and (HSC), Each concrete type was categorized into three groups subjected to temperatures of 400, 600, and 800 degrees Celsius for a duration of two hours.

2.3 Concrete Mixture and Specimen Preparation

In order to attain the required compressive strengths of 35 MPa and 55 MPa after 28 days of curing, the concrete mixes were made in compliance with ACI 211.1 criteria. An electric mixer was used to create homogenous concrete mixtures at the ratios [1:2.1:2.16:0.4+1.2 L/100kg of cement admixture] and [1:1.68:1.72:0.3+1.8 L/100kg of cement] [cement fine aggregate: coarse aggregate: W/C ratio admixture] for C-35 and C-55, respectively. To increase the concrete's water content efficiency, a chemical addition based on polycarboxylsic polymers was used, which produced a slump of 19.5 cm. In order to remove air spaces and ensure adequate compaction, specimens were cast in two layers using steel molds and then compressed using vibrating tables. Before being demolded, the specimens' upper surfaces were polished with a trowel and covered with sheets of polyethylene for a whole day. The samples were then submerged in a tank of water for 28 days to cure before to the incineration process.

Fig. 1. Concrete specimens' preparation

2.4 Heating Regime

In an electrical furnace, the cured concrete cylinders were heated to 400°C, 600°C, and 800°C for two hours at a rate of five degrees Celsius per minute. When the furnace reached the desired temperature, the retention time began. Following the heating phase, the furnace was switched off, and the specimens were left to cool within the furnace for 24 hours prior to reaching room temperature by air cooling [24,36].

Fig. 2. Electric furnace used to expose the specimens to elevated temperature

2.5 Uniaxial Compressive Strength Test

All post-cooled concrete cylinders were tested under uniaxial compression stress at the compression machine with a 2000 kN capacity, used to test the load capacity and stress-strain performance. All concrete cylinders were tested under uniaxial compression to measure the load capacity and stress-strain performance of the concrete columns. A compression testing machine was used to apply loads on the specimen, with the setup including a specialized ring for measuring the Modulus of Elasticity. This ring was equipped with a gauge to record lateral deformations. The test bolts were installed on the specimen at a height of 10 cm from the top and 10 cm from the bottom. Fig. 3 illustrates how the testing procedure is set up. In order to prevent premature collapse in the areas next to their ends, the columns were also constrained by steel rings at both ends.

Fig. 3. Testing setup for the uniaxial compressive strength test

2.6 Microstructure Test

2.6.1 Scanning Electron Microscopy (SEM)

The Scanning Electron Microscope (SEM) is frequently utilized for the observation of microstructural alterations and their consequences on fired concrete after high-temperature exposure. It also offers in-depth knowledge of the concrete pore structure, its cracks, and the chemical composition, thereby giving the means for researchers to make an estimation of the damage of the temperature-induced degradation and the condition of the structural integrity.

2.6.2 X-ray Diffraction (XRD)

This test serves as an essential method for examining the mineralogical and crystalline phases in concrete that has been fired or subjected to high heat. This technique helps identify alterations in the crystalline structure resulting from elevated temperatures, including the breakdown of calcium hydroxide (CH) and the emergence of new phases like calcium silicate phases (C-S-H) or portlandite. Such changes can provide insights into the temperature exposure history and the extent of damage to the material. Research indicates that XRD is especially effective in measuring phase changes due to thermal effects, such as the transformation of quartz or the decomposition of carbonates in concrete. By analyzing the intensity of diffraction peaks, the crystalline structure can disclose both the chemical composition and the degree of thermal degradation [13-18].

3. Result and Discussion

3.1 Visual Inspection

In the case of high temperatures, the different behaviors between C-35 and C-55 are observed. Their material is responsible rather than the properties in the structure, especially the W/C. At 400°C, both C-35 and C-55 maintain structural integrity with minimal surface degradation. Figure 4-a shows the surface exhibits homogeneity, and no significant cracks are evident. The material begins to lose bound water from the cement matrix. It marginally alters the interior microstructure. Figure 5-a illustrates C-55 cylinder that similarly does not show significant deterioration. However, due to a smaller water/cement ratio and gradually dense microstructure, its internal expansion caused by heating may develop micro-cracks that are not visible outside. At T600, the thermal damage becomes more distinct, varying between the two kinds of concretes. For C-35 specimens, the cracks and surface roughness reflect increased thermal expansion, leading to microstructural weakening. Decomposition of calcium hydroxide (Ca(OH)) initiates, further reducing its strength as shown in Fig.4-b. Also, C-55 Material is less harshly damaged from the surface compared to C-35, but its denser microstructure with lower porosity restricts further its capability for thermal expansion accommodation. The internal microcracks are probably formed and might further propagate under additional thermal or mechanical stress as illustrated in Fig.5-b Regarding T800, the magnitude of the thermal degradation for each type of concrete becomes significant.

(a) (b) (c) (d)

Fig. 4. Compressive strength tested specimens of C-35 cylinders after heating: (a)T400, (b) T600, (c) T800 before aging, (d) T800 after aging

In the case of C-35, the dominant features of the specimen are major spalling and surface cracks. Due to the decarbonation of the calcium carbonate, a severe loss in strength will result, together with the collapse of the cement matrix observed in Figure 4-c. For C-55 and at this point, despite the higher initial strength, the heat susceptibility of C-55 becomes either comparable or even more pronounced. Its dense structure, though desirable under normal conditions, is deleterious at high temperatures. The structural inability for internal dissipation of thermal stress leads to extended internal damage due to the confinement of expansion forces within the compacted matrix as depicted in Fig.5-c. Fig.4-d and Figure 5-d provide a visual representation of the concrete cylinders

heating to 800^0C, calcium carbonate ($CaCO_3$) undergoes decomposition, breaking down into calcium oxide (CaO) and carbon dioxide (CO_2), after aging and exposure to air, calcium oxide (CaO) starts absorbing moisture from the environment, forming calcium hydroxide ($Ca(OH)_2$).this reaction leads expansion which induces internal stresses and further cracking. Over time, these cracks propagate, causing the surface layers to crumble and the aggregate to detach from the cement matrix, as seen in the image.

(a) (b) (c) (d)

Fig. 5. Compressive strength tested specimens of C-55 cylinders after heating: (a)T400, (b) T600, (c) T800 before aging, (d) T800 after aging

3.2 Mechanical Properties of Concrete at Elevated Temperatures

The average of three specimens for Compressive strength and axial strain test results per temperature per concrete type of the heated concrete cylinders are shown in Table 1. As the temperature rises up to T400, it significantly decreases to 28.7 MPa, which is apparently a reduction of about 22.4%, presumably due to certain changes in microstructure consisting of cement paste and aggregate. When further heated to T600, the strength decreases drastically to 14.2 MPa, which is about 61.5% lower than the initial strength. A probable reason for degradation may be due to not only the chemical decomposition of calcium hydroxide but also the formation of cracks. Whereby, the compressive strength drops to 7.6 MPa for a temperature of T800, representing an accumulated loss of about 79.3%, revealing significant structural damage characterized by heavy material degradation. Regarding Axial Strain, under this tensile deformation, at ambient conditions, the axial strain at T25 is 0.322 mm. Interestingly, at T400 it increases significantly to 0.75 mm, indicating supposedly increased ductility through the weakening of the internal bonds. At T600, the strain drops to 0.111 mm, which may reflect that the mechanisms of brittle failure have prevailed under the deterioration of integrity in the material. It is followed by the rebounding of the strain up to 0.54 mm at T800, most probably due to the combined effect of strong cracking and residual ductility of the degraded structure.

Table 1. Ultimate compressive stress and axial strain of the tested columns

Heating Degree	Compressive stress (MPa)	S.D (MPa)	Axial.strain (mm)	S.D (mm)
a. compressive strength 35 MPa				
T25	36.90	0.60	0.00322	0.113
T400	28.70	0.50	0.0075	0.0424
T600	14.20	0.42	0.00111	0.0141
T800	7.60	0.28	0.0054	0.0141
b. compressive strength 55 MPa				
T25	59.20	1.13	0.00468	0.009
T400	31.60	0.57	0.00115	0.0099
T600	20.60	0.71	0.016	0.0283
T800	8.9	0.33	0.0033	0.0121

In Table 1.b, compressive strength 55 MPa, the strength at the state of T400 drops drastically to 31.6 MPa, about a 46.6% reduction, reflecting a higher susceptibility of C-55 to elevated temperatures. By T600, a further reduction of compressive strength to 20.60 MPa, about a cumulative loss of 65.2%, was obtained probably for similar thermal damage mechanisms developed in lower strength concrete. On the other hand, the compressive strength goes to 8.9 MPa at T800, which means complete failure in structural integrity. The axial Strain at T400 grossly drops to 0.115 mm; this actually reflects that at this temperature, it acts in a more brittle way. From T600, due to the break of bonds and increased deformation under load, the strain increases up to 1.6 mm. This strain would correspond with 0.0033 mm at T800, indicating approximately a complete loss of compressive strength and structural collapse. According to the above result, higher-strength concrete is more vulnerable to thermal damage, whereas the higher paste content and denser microstructure in C-55contribute to increased susceptibility due to thermal expansion mismatch and increased pore pressure. Also, thermal incompatibility between aggregate and cement paste causes internal cracking and further deterioration. As a result, Compressive strength loss accelerates beyond T400 and becomes severe at T600-T800 due to chemical decomposition and microcracking and Axial strain decreases sharply beyond T600, indicating a transition from ductile to brittle failure mechanisms [20,21,35].

3.3 Stress-Strain Behavior

The stress-strain curves in Fig.6 illustrate the mechanical behavior of concrete cylinders with compressive strengths of 35 MPa and 55 MPa during high temperatures. It shows the effect of thermal exposure on the matter's stress-strain relationship. The temperature will affect the stress-strain behavior of the C-35 concrete cylinders. The curve at 25°C, at room temperature, has higher stiffness and maximum stress, showing superior mechanical performance. At T400, the ultimate stress is somewhat reduced with increased strain at failure, showing reduced stiffness. At T600, the decrease in ultimate stress is quite significant, coupled with further increases in strain at failure, indicating considerable thermal degradation. At T800, the stress-strain curve flattens out further, reflecting a significant loss in both strength and ductility owing to extensive thermal damage. In the case of C-55 concrete cylinders, a similar trend is observed. At T25, the concrete is very stiff and strong and reaches its maximum stress at lower strains. At T400, the ultimate stress decreases while the strain capacity increases, showing a loss of stiffness. While the stress-strain curve for the material tested at T600 gives further strength reduction and an evident increase of strain at failure, revealing the effects of thermal damage on high-strength concrete, at T800 it shows a great fall in strength and stiffness. It can be seen from this that, with a less steep slope of the curve, there is advanced thermal degradation in this material. Both concrete grade trends point out that thermal exposure acts to the detriment of concrete's mechanical performance. The result draws attention to the fact that taking the effect of temperature in design and analysis cannot be disregarded for concrete structures that might undergo high-temperature levels—for example, those that are subjected to fire conditions [8,20-25,36].

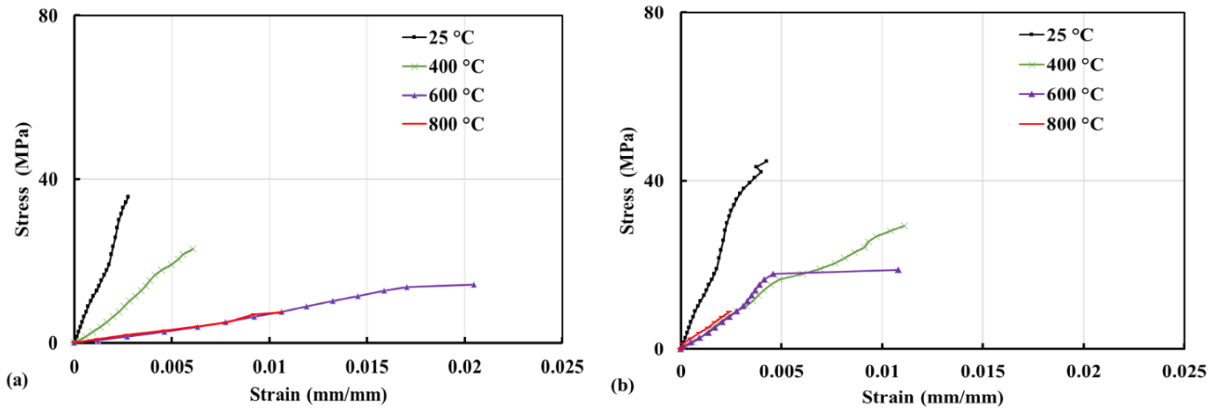

Fig. 6. Stress-strain curves of NSC (35 MPa) and HSC (55 MPa) at different temperature levels

3.4 Microstructure Tests

3.4.1 Scanning Electron Microscope

Evaluation of the possible changes in the microstructural features in the fracture surface of concretes, could be useful to explain the changes in the compressive strengths due to exposure to heating effects. In the present work, a Scanning Electron Microscope (SEM) was executed to distinguish such probable relations. SEM images of both C-35 and C-55, 28-day age, at T25 , T400 , and T800 are presented in Figures 7 and 8, respectively. For C-35 Figure 7-a showed that before exposure to high temperatures, the fracture surface was dense and lacked visible pores or cracks. The images also displayed a matrix with intertwined string-like structures. When the temperature reached T400, spalling began due to water evaporating from the capillary pores. This process started at 100°C, where both free and absorbed water gradually disappeared. As dehydration occurred, crystalline structures became more visible, but noticeable microcracks had not yet developed at this stage. At 500°C, the concrete lost all calcium hydroxide ($Ca(OH)_2$). At this point, distinct structural changes were observed as shown in Figure7-b, caused by the breakdown of hydration products under heat. By T800, the surface began to disintegrate as illustrated in Figure 7- c. This happened because calcium silicate hydrate (C-S-H) phases broke down chemically, releasing the water that had been chemically bound. This caused widespread microcracking and internal fissures to form throughout the concrete. The material's structural integrity was significantly weakened, leading to fragmentation and the collapse of its microstructure.

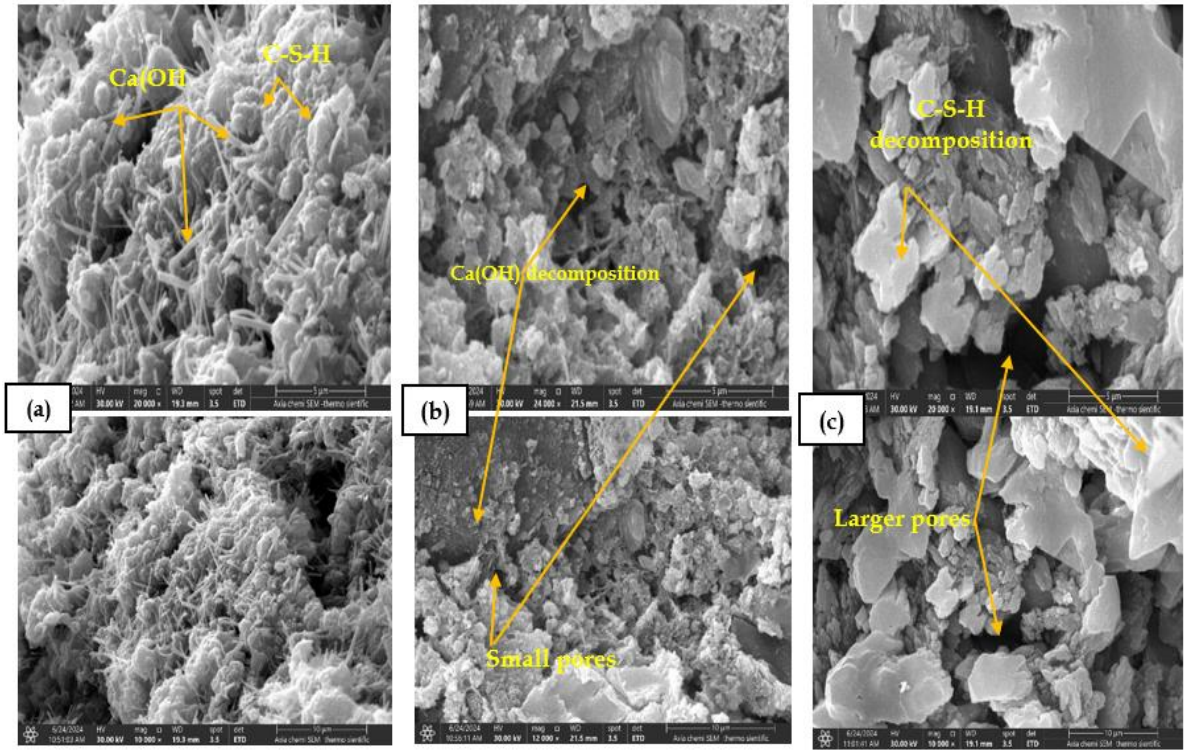

Fig. 7. SEM image for concrete with 35 MPa compressive strength, exposed to: (a) T25, (b) T400 , (c) T800

Concrete durability depends on the amount of the phase and microstructure constituents formed during the hydration reaction primarily. From the microstructure of the 55 MPa concrete sample at ambient temperature (i.e. T25), it is possible to observe a dense and compact matrix with a negligible volume of pores or cracks, which impedes the mechanical interlocking of pore structures. The images also presented a matrix with intertwined needle-like structures. The physical alteration of the concrete microstructure is appreciable only beyond this temperature, primarily due to the combination of decomposition of several hydration products including the formation of two dehydroxylated compounds and evaporation of water in its free and capillary forms which weakens the bond formed between aggregates and self-locked products. Predominantly, efficient interfacial

transition zones and crystals emerged within and in between cement blends in the pores, aiding in garnering decent mechanical strength for the samples as observed in Figure 8-a.

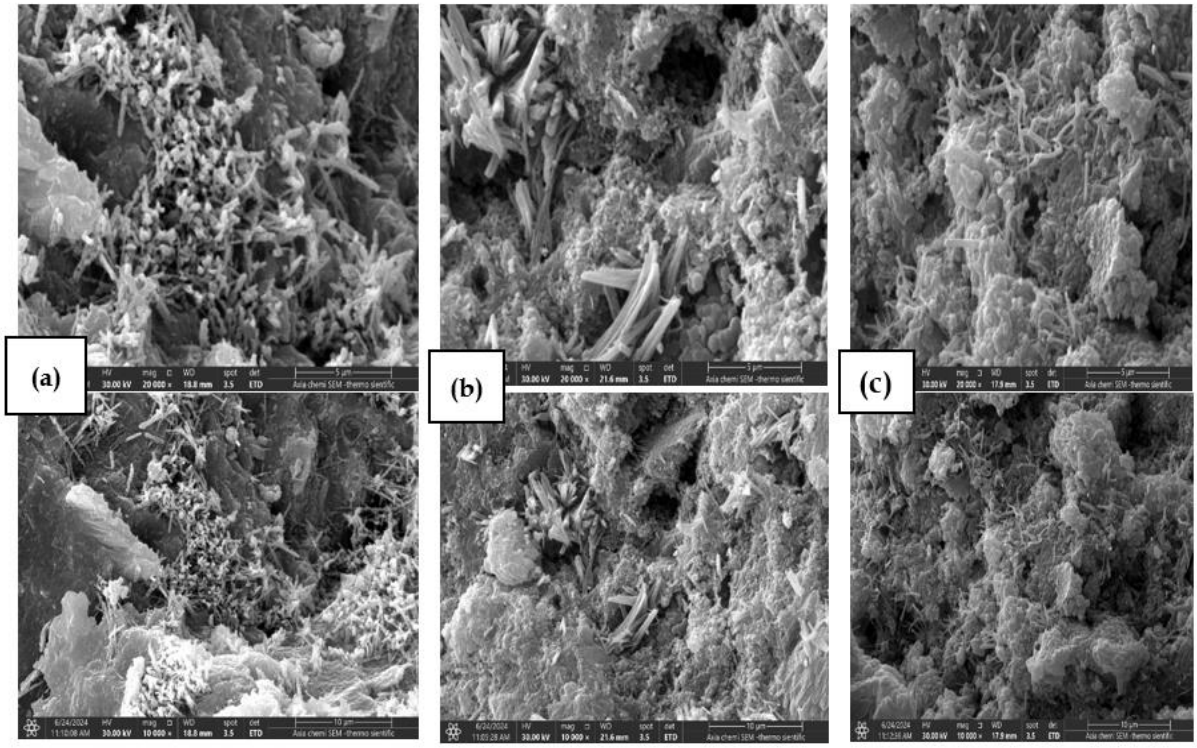

Fig. 8. SEM image for concrete with 55 MPa compressive strength, exposed to: (a) T25 , (b) T400, and (c) T800

Concrete with a 55MPa compressive strength shows marked microscopic alterations and ranges between moderate and high porosity when heated to T400. This is an immediate cause for the agglomeration of C-S-H and vinyl polymers that leads to microscopic flaking and cracking due to the shrinking and tensile stress. In place of $Ca(OH)_2$, it is apparent that these isotopic remnants are crystallites that manifest appreciably after chemically bonded water is evaporated. Notable temperature increases on attire structural arrangement, i.e. microscopic cracks, was however absent in the appearance of the grain after heating and shown in Fig. 8-b. This finding is consistent with others [26,27].

3.4.2 X-ray Diffraction (XRD)

The X-ray diffraction (XRD) curves of the two types of concretes, C-35 and C-55, before heating (i.e. at T25) and after being subjected to different heating temperatures, T400 and T800 are presented in Figs. 9 and Figure 10, respectively. In general, the crystal phase of the tested specimens changes remarkably after exposure to high temperatures. At T25 (i.e. before heating), in the C-35 concrete (Figure 9), the CH diffraction peak intensity is comparable to that of C-55 concrete Figure 10. This result suggests that concrete grade has no impact on the formation of the CH hydrate as long as the solid proportions of both types are similar. When the temperature was raised to T400 , the internal autoclaving conditions of the concretes accelerated the hydrations, which improved the matrix microstructure [28-32]. At T800, the diffraction peaks of portlandite (CH) disappeared, revealing that the portlandite (CH) phase dehydrates at elevated temperatures. Moreover, in both concretes, C-35 and C-55, extra calcium oxide (CaO) is produced, due to the decomposition of CH. Therefore, high crystalline phase peaks of gehlenite ($Ca_2Al_2SiO_7$) and wollastonite ($CaSiO_3$) were observed in both concrete specimens. However, this increase was more pronounced in C-55 type, which has a lower w/b ratio. Wollastonite Gehlenite is generated due to the potential reaction of calcium oxide with Al_2O_3 and SiO_2 hydrates exist in cement particles at temperatures more than T800[32,33], as they consist of an aluminosilicate skeleton structure [29]. In addition, quartz available in silica sand particles reacts with CaO due to exposure to elevated temperature, leading to the formation of calcium silicate (C_nS) phase [29,32]. This phase can also be generated due to the decomposition of CSH. In general, after exposure to elevated temperatures up to 800°C, the main phases observed in

both concretes, C-35 and C-55, are calcium silicate, Gehlenite, and quartz. This observation is agreed with others [29].

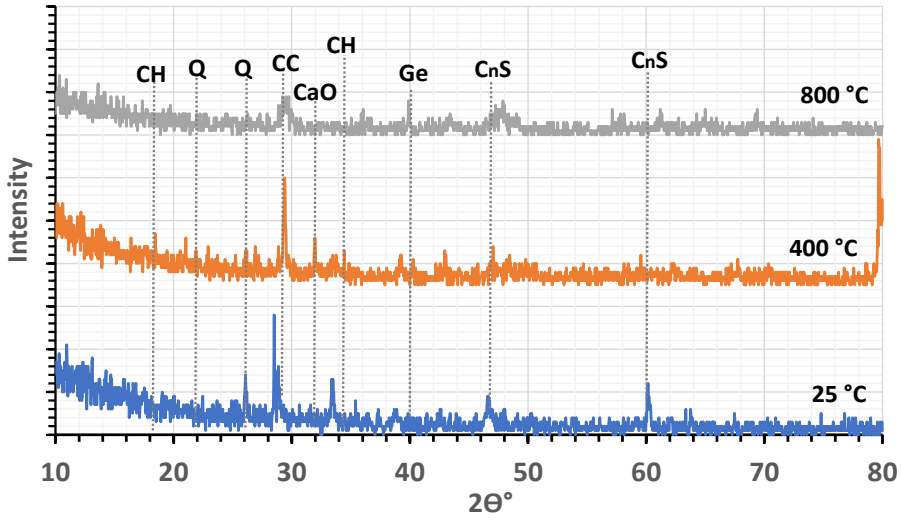

Fig. 9. XRD patterns of C-35 concrete obtained at T25 , T400, and T800

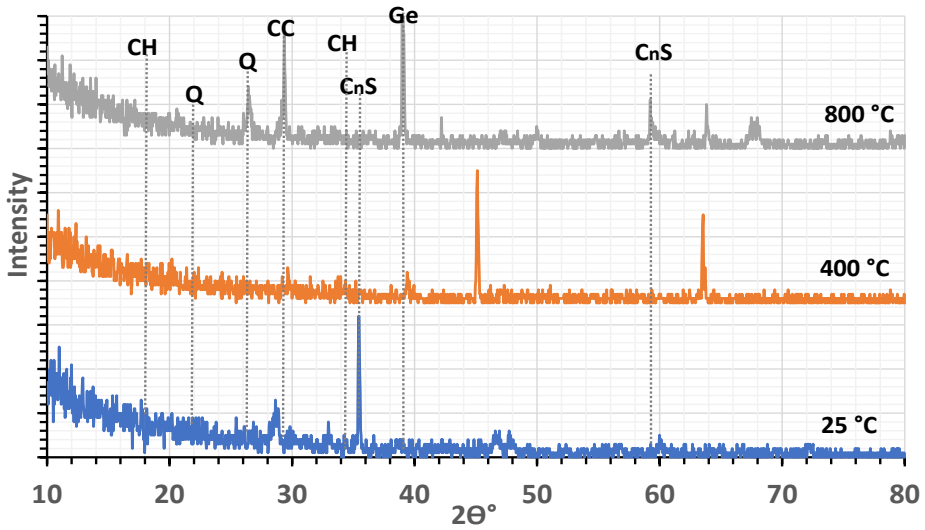

Fig.10. XRD patterns of C-55 concrete obtained at T25 , T400, and T800

4. Conclusions

The elevated temperature can be a vulnerable factor in concrete structures. This paper studied the effect of high temperatures on both NS and C-55. The following conclusions can be drawn:

- Concrete of higher initial compressive strength, 55 MPa, has bigger absolute losses of strength with the increase of temperature; it retains, however, a higher percentage up to T400, where beyond this point, degradation accelerates.
- Both types of concretes have shown a gradual reduction in strength up to an increased temperature, while experiencing a steeper decrease beyond T400. Strain data shows that C-55makes its transition to a brittle mode of failure more rapidly than the lower-strength concrete, particularly in the intermediate temperature range.
- The losses in strength and strain capacity observed at T800 for the two mixes confirm that very high-temperature changes may severely affect the ability of concrete to resist load, and therefore, protective measures should be taken in cases where the concrete serves in a fire-hazardous environment.
- Temperature increases concrete vulnerability, reducing compressive strength and ductility. Higher-strength concretes become brittle, posing structural challenges.

- The SEM analysis revealed significant microstructural changes in both C-35 and C-55 due to temperature elevation. C-35 experienced spalling and dehydration at T400, while C-55 maintained a dense structure at T400 but experienced porosity and agglomeration at 800°C. These findings are crucial for designing fire-resistant and durable structures.
- The crystal phase of the tested concretes resulted from XRD changes remarkably after exposure to high temperatures. At T25 , the CH diffraction peak intensity is comparable for both concrete types. This result suggests that concrete grade has no impact on the formation of the CH hydrate as long as the solid proportions of both types are similar. Calcium silicate, Gehlenite, and quartz are the primary phases seen in both C-35 and C-55 concretes following exposure to high temperatures up to T800.
- For producing fire-resistant concrete, using aggregates that are resistant to fire and adding SCMs (e.g. fly ash) will enhance the performance. Also, adding Polypropylene will be an advantageous procedure to reduce spalling. In terms of structure, increasing concrete cover and using corrosion-resistant rebar also improve heat protection, and larger cross-sections delay heat penetration. Intumescent coatings help to delay heat transfer. Finally, rigorous testing and standardization are essential for ensuring fire resistance. Fire resistance tests, such as those specified by ISO 834 and ASTM E119, help verify the structural integrity of concrete exposed to elevated temperature. Numerical modeling can also be used to predict the fire performance of concrete designs, aiding in the development of guidelines for fire-resistant construction and rehabilitation strategies.
- For future research, it will be beneficial to study the various rehabilitation techniques for concrete structures damaged by fire. Rehabilitation techniques like the application of carbon fiber-reinforced polymer fabrics may improve the post-fire reduction in mechanical properties. Moreover, employing novel composite or hybrid materials as other innovative rehabilitation techniques, may enhance the performance of concrete exposed to extreme temperatures.

References

[1] American Concrete Institute (ACI). Code requirements for determining fire resistance of concrete and masonry construction assemblies (ACI 216.1-07/TMS-0216-07). Farmington Hills (MI): ACI; 2019.
[2] American Concrete Institute (ACI). Building code requirements for reinforced concrete and commentary (ACI 318). Farmington Hills (MI): ACI; 2025.
[3] European Committee for Standardization. EN 1991-1-2: Actions on structures - Part 1-2: General actions - Actions on structures exposed to fire (Eurocode 1). Brussels: CEN; 2024.
[4] Abdul-Hameed AH, Mansi SA, Hassan MS. Factors affecting compatibility between (S.B.R) polymer repair materials and concrete substrate. Eng Technol J. 2010;28(14):4853-65. https://doi.org/10.30684/etj.28.14.14
[5] European Committee for Standardization. EN 1992-1-2: Design of concrete structures - Part 1-2: General rules - Structural fire design (Eurocode 2). Brussels: CEN; 2004.
[6] Kodur V. Properties of concrete at elevated temperatures. ISRN Civ Eng. 2014;2014:468510. https://doi.org/10.1155/2014/468510
[7] Purkiss JA. Fire safety engineering design of structures. Oxford: Butterworth-Heinemann, Elsevier; 2007. https://doi.org/10.1201/b12845
[8] Kodur VR, Raut N. Performance of concrete structures under fire hazard: Emerging trends. Indian Concr J. 2010;84(2):23-31.
[9] ASTM International. ASTM E119-08b: Standard test methods for fire tests of building construction and materials. West Conshohocken (PA): ASTM; 2024.
[10] Khoury GA, Majorana CE, Pesavento F, Schrefler BA. Modelling of heated concrete. Mag Concr Res. 2002;54(2):77-101. https://doi.org/10.1680/macr.2002.54.2.77
[11] Poon CS, Shui ZH, Lam L. Compressive behaviour of fiber reinforced high-performance concrete subjected to elevated temperatures. Cem Concr Res. 2004;34:2215-22. https://doi.org/10.1016/j.cemconres.2004.02.011
[12] Hertz KD, Sørensen LS. Test method for spalling of fire exposed concrete. Fire Saf J. 2005;40(5):466-76. https://doi.org/10.1016/j.firesaf.2005.04.001
[13] Fernandes B, Masiero Gil A, Longhi Bolina F, Fonseca Tutikian B. Thermal damage evaluation of full-scale concrete columns exposed to high temperatures using SEM and XRD. Dyna. 2018;85(207):123-8. https://doi.org/10.15446/dyna.v85n207.70593

[14] Mansi AS. Bond strength assessment for different types of repair materials. Eng Technol J. 2010;28(21):6325-36. https://doi.org/10.30684/etj.28.21.10
[15] Mansi AS, Abdulhameed HA, Yong YK. Development of low-shrinkage rapid set composite and simulation of shrinkage cracking in concrete patch repair. In: Proc Int Conf Transportation and Development 2018; 2018 Jul; Reston (VA). Reston (VA): ASCE; 2018. p. 215-26. https://doi.org/10.1061/9780784481554.022
[16] Alhasanat MB, Al Qadi AN, Al Khashman OA, Dahamsheh A. SEM evaluation of self-compacting concrete spalling at elevated temperatures. Am J Eng Appl Sci. 2016;9(1):119-27. https://doi.org/10.3844/ajeassp.2016.119.127
[17] Kang WL. Application of SEM and XRD in the microstructure analysis of fiber-reinforced concrete corroded by salt solution. Adv Res. 2024;25(6):336-42. https://doi.org/10.9734/air/2024/v25i61207
[18] Balakrishnaiah D, Balaji KVGD, Srinivasa RP. Application of SEM method to investigate the effect of elevated temperatures on compressive strength of ternary blended concrete. ARPN J Eng Appl Sci. 2017;12(7):2029-36.
[19] Yuzer N, Akoz F, Ozturk LD. Compressive strength-colour change relation in mortars at high temperature. Cem Concr Res. 2004;34:1803-7. https://doi.org/10.1016/j.cemconres.2004.01.015
[20] Li G, Feng L, Zheng S. Investigation on the properties of concrete and its composites after exposure to high temperature. Sichuan Build Sci. 1991;2:1-5. Chinese.
[21] Hu H, Dong Y. Experimental research on strength and deformation of high-strength concrete at elevated temperature. China Civ Eng J. 2002;35:44-7. Chinese.
[22] Bamonte P, Gambarova PG. Mechanical properties of self-compacting concrete at high temperature and after cooling. Mater Struct. 2012;45(9):1375-87. https://doi.org/10.1617/s11527-012-9839-9
[23] Huo JS, He YM, Xiao LP, Chen BS. Experimental study on dynamic behaviours of concrete after exposure to high temperatures up to 700°C. Mater Struct. 2013;46:255-65. https://doi.org/10.1617/s11527-012-9899-x
[24] Ma Q, Guo R, Zhao Z, Lin Z, He K. Mechanical properties of concrete at high temperature: A review. Constr Build Mater. 2015;93:371-83. https://doi.org/10.1016/j.conbuildmat.2015.05.131
[25] Al-Sulayfani JB, Al-Taee HT. Modeling of stress-strain relationship for fibrous concrete under cyclic loads. Eng Technol J. 2008;26(1):45-54. https://doi.org/10.30684/etj.26.1.4
[26] Annerel E, Taerwe L. Revealing the temperature history in concrete after fire exposure by microscopic analysis. Cem Concr Res. 2009;39(12):1239-49. https://doi.org/10.1016/j.cemconres.2009.08.017
[27] Amiri M, Aryanpour M, Porhonar F. Microstructural study of concrete performance after exposure to elevated temperatures considering C-S-H nanostructure changes. High Temp Mater Process. 2022;41(1):224-37. https://doi.org/10.1515/htmp-2022-0030
[28] Farage MCR, Sercombe J, Gallé C. Rehydration and microstructure of cement paste after heating up to 300 °C. Cem Concr Res. 2003;33:1047-56. https://doi.org/10.1016/S0008-8846(03)00005-X
[29] Lin RS, Han Y, Wang XY. Macro-meso-micro experimental studies of LC3 paste subjected to elevated temperature. Cem Concr Compos. 2021;116:103871. https://doi.org/10.1016/j.cemconcomp.2020.103871
[30] Albeer SJ, Hassan MS. Microstructure and strength of nanosilica- and microsilica-enhanced mortars under elevated temperatures. Arab J Sci Eng. 2024;49(4):5565-77. https://doi.org/10.1007/s13369-023-08430-3
[31] Hassan MS, Al-Azawi ZM, Taher MJ. Complementary effect of heat treatment and steel fibers on properties of high-performance concrete. Arab J Sci Eng. 2016;41(10):3969-81. https://doi.org/10.1007/s13369-016-2056-z
[32] Traoré K, Kabré TS, Blanchart P. Gehlenite and anorthite crystallisation from kaolinite and calcite mix. Ceram Int. 2003;29:377-83. https://doi.org/10.1016/S0272-8842(02)00148-7
[33] Alani S, Hassan MS, Jaber AA, Ali IM. Effects of elevated temperatures on mortar containing nano-calcined montmorillonite clay. Constr Build Mater. 2020;263:120895. https://doi.org/10.1016/j.conbuildmat.2020.120895
[34] Mussa MH, Hason MM, Abdulhameed HA. Fire simulation of RC slab inclusion with nano-silica and high-volume fly ash. In: AIP Conf Proc. 2022 Nov;2660(1). https://doi.org/10.1063/5.0109533
[35] Thanaraj DP, Kiran T, Kanagaraj B, Nammalvar A, Andrushia AD, Gurupatham BGA, et al. Influence of heating-cooling regime on engineering properties of structural concrete. Buildings. 2023;13(2):295. https://doi.org/10.3390/buildings13020295
[36] Cheng FP, Kodur VKR, Wang TC. Stress-strain curves for high-strength concrete at elevated temperatures. J Mater Civ Eng. 2004;16(1):84-90. https://doi.org/10.1061/(ASCE)0899-1561(2004)16:1(84)
[37] Soroushian P, Won JP, Hassan M. Sustainable processing of cellulose fiber cement composites. ACI Mater J. 2013;110(3). https://doi.org/10.14359/51685664